Development of a Fast Gain Tilt Compensator

by Tatsuya Hatano *, Daeyoul Yoon * and Kazuyou Mizuno *

ABSTRACT   In designing a network architecture to offer greater flexibility and higher reliability in the wavelength-division multiplexing (WDM) systems of the future, an architecture that uses the optical add-drop multiplexer (OADM) for signal I/O with respect to the transmission path has been proposed. It is known that changes in the gain of the erbium-doped fiber amplifier (EDFA) that accompany fluctuation in the signal light input to the OADM and changes in Raman gain generated in the transmission path occur in the sub-millisecond order. It is also known that this gain change is gain tilt occurring in the wavelength direction, constituting a factor in the degradation of transmission characteristics due to the power level deviations among signals. We have developed a fast gain tilt compensator that is capable of operation in the microsecond order and uses a lithium niobate (LN) polarization transformer to compensate for the gain tilt due to these gain changes.

1.   INTRODUCTION

The larger volume and faster speed of data transmission due to the rapid spread of Internet services has resulted in active research efforts being devoted to wavelength division multiplexing (WDM) systems. In designing a network architecture to offer greater flexibility and higher reliability for the wavelength-division multiplexing (WDM) systems of the future, an architecture that uses the optical add-drop multiplexer (OADM) for signal I/O with respect to the transmission path has been proposed.

It is known that changes in the gain of the erbium-doped fiber amplifier (EDFA) that accompany fluctuation in the signal light input to the OADM and changes in Raman gain generated in the transmission path occur in the sub-millisecond order [1].

Figure 1 is a block diagram showing a transmission system with an OADM, from which it may be seen that when the number of signals input to the OADM is reduced due to fiber breakage etc., there will be a change in Raman gain in the transmission fiber caused by stimulated Raman scattering (SRS). It is known that the gain change constitutes a gain tilt generated in the wavelength direction, and it is a factor in the degradation of transmission characteristics due to power level deviations among signals. A variety of methods have been proposed for achieving gain tilt compensation.

Among these compensation methods are gain tilt adjustment by controlling the internal pump laser light source of the EDFA, flattening of the output power level by means of a variable optical attenuator, and a technique

that compensates for the gain tilt using a gain tilt compensator (GTC) that can vary the slope of the wavelength-transmittance characteristic by means of control parameters, as shown in Figure 2. Of these the GTC seems promising, due to the fact that is capable of batch compensation of the band used and because the compensa-
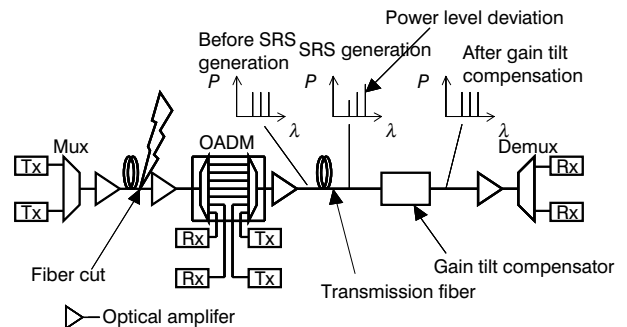

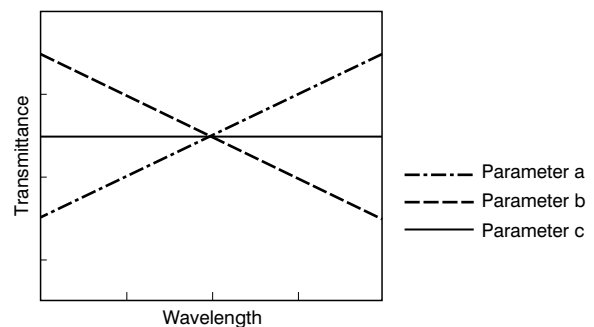**Figure 1   Block diagram of a transmission system with an OADM.**

Figure 2   Change in slope of transmittance characteristics of a variable GTC.

* Optical Transmission Components Development Dept., FITEL-Photonics Lab., R&D Div.

tion width is large, thereby reducing system cost.

As of the present time, techniques proposed to construct a GTC include a method that uses a Faraday rotator [2], and a technique that uses a heating means (heater, etc.) to vary the slope of the wavelength-transmittance characteristic of a Mach-Zehnder circuit on a planar waveguide using a material like silica glass etc [3].

Neither, however, has been able to follow gain changes occurring at the sub-millisecond order. Accordingly, in order to compensate for the gain tilt due to changes in gain occurring at the sub-millisecond order, we have developed a GTC using a lithium niobate (LN) polarization transformer that is capable of operating at the microsecond order.

2. PRINCIPLE AND CONFIGURATION

In this section we discuss the principle by which a transmittance slope waveform is generated, and describe an LN polarization transformer.

2.1 Principle of Transmittance Slope Generation

Figure 3 shows the principle of generation of transmittance slope in this GTC. When linear polarized light in the X-axis direction impinges on a doubly refracting crystal, a retardation Δ dependent on the wavelength is generated between the orthogonally polarized components of the incident light. Figure 4 shows optical output power P for a case in which the light having this retardation Δ impinges on the polarizer and only that polarized component of a given direction is extracted. Figure 4 shows the transmit-
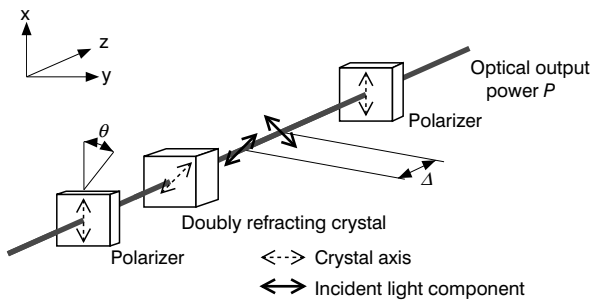
tance characteristics when the input-side polarizer angle θ shown in Figure 3 is 0, 45 and 90° with a dashed line, solid line and dot-dash line respectively.

Optical output power P varies sinusoidally with respect to retardation Δ. Further the amplitude of the sinusoidal wave can be controlled by changing the state of polarization of light incident on the doubly refracting crystal, making it possible to change the slope centered at the wavelength that is the node. The state of polarization of the incident light is changed by an LN polarization transformer, which is described in Section 2.2 below. The retardation Δ (wavelength) that constitutes the node in Figure 4 sets the range of retardation Δ (wavelength) used and determines the length of the doubly refracting crystal, thereby making control possible.

2.2 LN Polarization Transformer

Figure 5 is a schematic diagram of the LN polarization transformer used in this GTC. It is made of an X-cut LN crystal substrate measuring 4.5 × 20.5 × 0.5 mm. As the figure shows, when a voltage is applied in the X-axis direction of the LN crystal, the refractive index of the LN crystal axis changes in accordance with the electro-optical effect. Taking advantage of this it is possible to change the state of polarization of the incident light that propagates in the Z direction. The LN transformer is fabricated by depositing an SiO_2 buffer layer on the voltage application plane of the LN crystal, and an Au film is deposited on the both faces to make electrodes.

Figure 6 shows the change in the refractive index ellipsoid of an LN polarization transformer under applied volt-

Figure 3 **Principle of transmittance slope generation using a doubly refracting crystal.**

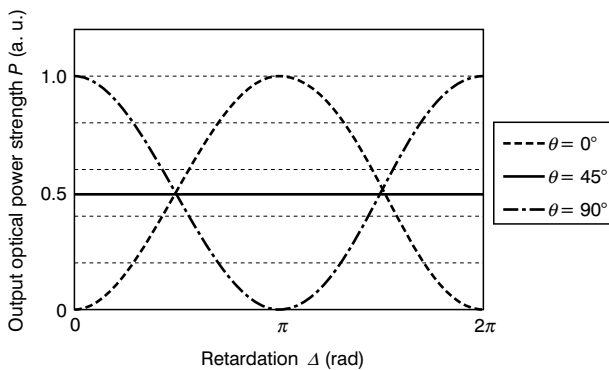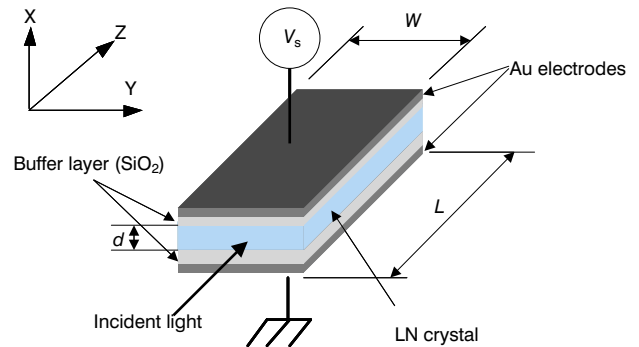**Figure 4** **Typical transmittance characteristics obtained by polarization manipulation using doubly refracting crystal.**

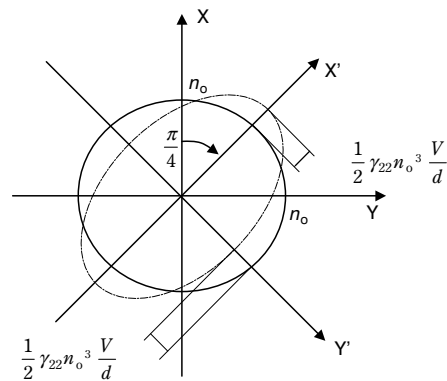**Figure 5** **Schematic diagram of LN polarization transformer.**

Figure 6 **Change in the refractive index ellipsoid of an LN polarization transformer under applied voltage.**

age. Here, assuming that the polarization state of the incident light is the X-axis direction of the LN crystal, when there is no voltage applied to the LN crystal, the polarization state does not change and the light is output as is. When there is a voltage applied to the LN crystal, a portion of the incident light is transformed to the Y-axis direction and when the retardation generated by the LN crystal becomes π, it becomes equivalent to a $\lambda/2$ waveplate disposed at an axis angle of 45°, and complete polarization transformation from the X-axis angle to the Y-axis angle is carried out.

The retardation Δ generated in the two major axis directions is given by

$$\Delta = \frac{2\pi}{\lambda}\gamma_{22}{n_0}^3\frac{V}{d}L \tag{1}$$

where λ represents the wavelength of the incident light, and by using the characteristic values for the LN crystal (namely electro-optical coefficient γ_{22} (5.4 pm/V), refractive index n_0 (2.14), thickness d and length L), and taking the applied voltage as V, we can find the retardation Δ. At a wavelength of 1.55 μm, voltage V_π at which retardation Δ is π will be 366 V.

Figure 7 shows the results of measuring V_π. In this evaluation a light linearly polarized in the X-axis direction is input to the LN polarization transformer, and only the component of the output light polarized in the X-axis direction was transmitted using the polarizer to be measured for its power under changing applied voltage V, and the applied voltage when the extinction ratio reached a maximum was taken as V_π. As can be seen from Figure 7, the extinction ratio reached its maximum at an applied voltage of 350 V, substantially agreeing with the calculated value. Note that the voltage applied to the prototype GTC module fabricated in this work ranged from –70 V to +70 V.

2.3 Configuration

Figure 8 is a schematic showing the structure of the GTC. The optical components of which it is made are the input and output collimators, rutile, a $\lambda/2$ waveplate (axis angle 22.5°), $\lambda/4$ waveplate (axis angle 0°), $\lambda/4$ waveplate (axis angle 90°), LN polarization transformer, and a quartz crystal and LN crystal forming a high-order waveplate.
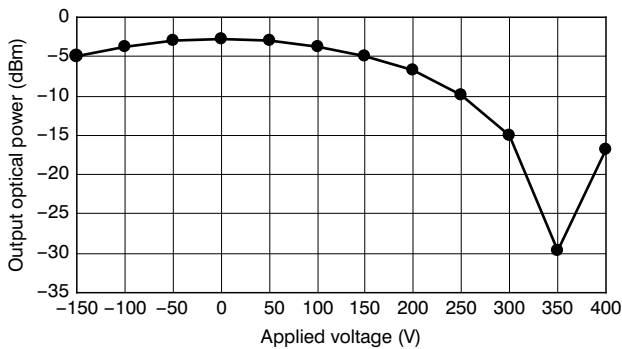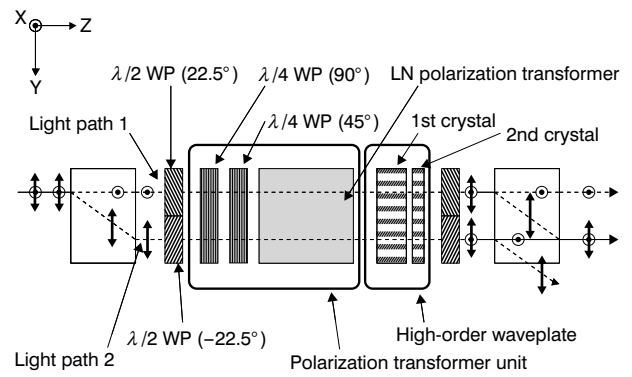

Figure 8 Schematic diagram of fast gain tilt compensator (GTC).

The incident light is separated by a polarization beam splitter into light path 1 and light path 2, both of which are in the same polarization state due to their respective $\lambda/2$ waveplates, and by passing through the polarization transformer unit are subjected to change in polarization associated with the applied voltage. Then, after impinging on the high-order waveplate that generates the sinusoidal waveform of the transmittance, only a portion of the polarized component is output. The polarization transformer unit comprises the LN polarization transformer and two $\lambda/4$ waveplates, of which the one whose axial direction is tilted at 45° to the X-axis direction is given an applied voltage offset such that when the applied voltage is 0 V, the amount of transmittance slope is 0. The high-order waveplate comprises a combination of crystals of two kinds—quartz and LN. The ratio of the respective crystal lengths is optimized, to cancel the temperature characteristics of the crystals. And the lengths of light path 1 and light path 2 are the same, in a structure that is so designed that polarization mode dispersion (PMD) does not occur.

Figure 9 shows the ideal transmittance characteristics of the GTC, in which λ_1, λ_2, λ_3, λ_4, and λ_5 are the wavelengths at which the retardation at the high-order waveplate are $-\pi$, $-\pi/2$, 0, $\pi/2$, and π.

It was so arranged that at wavelength λ_2, transmittance at an applied voltage of 0 V was 1.

Using one part of the C-band wavelengths, we were able to change the slope of the transmittance characteristic by changing the applied voltage.
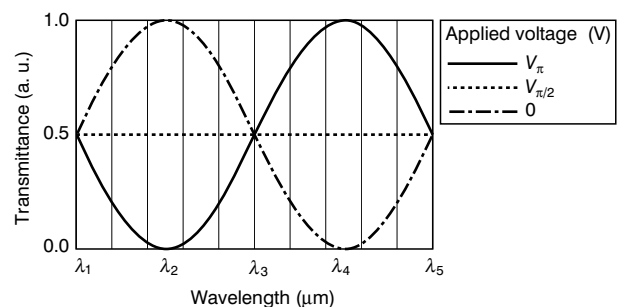

Figure 7 Measured values of the extinction ratio for LN polarization transformer.

Figure 9 Ideal transmittance characteristics of GTC.

3. PROTOTYPING RESULTS

3.1 Transmittance Characteristics

Figure 10 shows the wavelength vs. transmittance characteristics of the GTC module that we fabricated in this work. When the applied voltage was varied to −70 V, 0 V and +70 V, the slope of the transmittance characteristic changed, and at a center wavelength of 1553 nm, transmittance was −3.5 dB.

3.2 Linearity of Transmittance Characteristic

Figure 11 plots ripple against the slope of the transmittance characteristic for the prototyped GTC module, where the slope and ripple of the transmittance characteristic are defined as shown in Figure 12.

At a slope of 0.093 dB/nm, ripple was a maximum of 0.36 dB for the prototyped GTC module.

3.3 Relationship between Applied Voltage and Slope of Transmittance Characteristic

Figure 13 shows the relationship between applied voltage and the slope of the transmittance characteristic for the prototyped GTC module. At slopes of 0.094 dB/nm and −0.093 dB/nm, the applied voltages were −70.1 V and +68.4 V respectively.

3.4 Response Characteristic

Figure 14 shows values measured for the response of the wavelength vs. transmittance characteristic to changes in applied voltage. In the evaluation, the total optical output of the module was detected by photodiodes and convert-
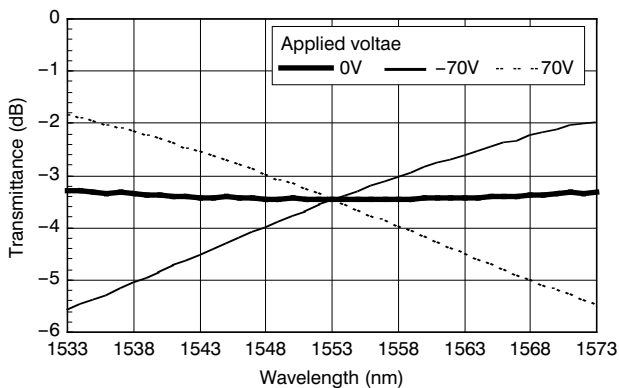

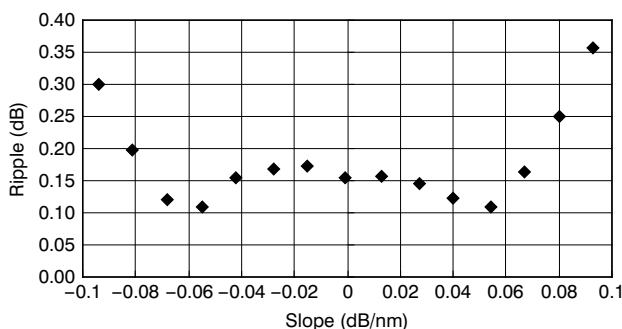**Figure 10 Transmittance characteristics of prototyped GTC module.**

Figure 11 Ripple in transmittance characteristics for prototyped GTC module.

$$\text{Slope} = b/a$$
$$\text{Ripple} = |\Delta_{min}| + |\Delta_{max}|$$
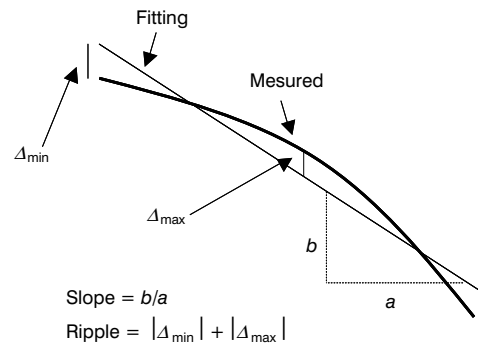
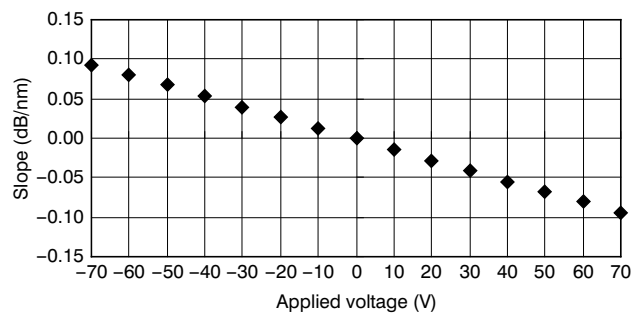**Figure 12 Definition of slope and ripple of transmittance characteristics.**

Figure 13 Relationship between applied voltage and slope of transmittance characteristic for prototyped GTC module.
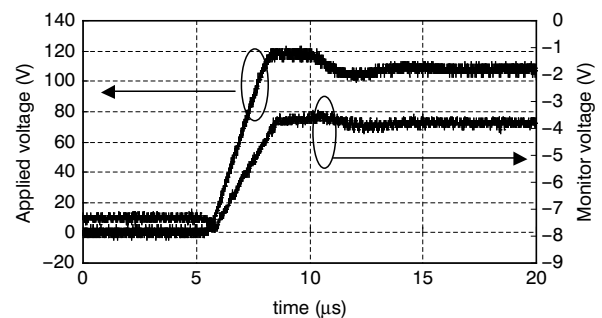

Figure 14 Response of transmittance characteristic to change in applied voltage.

ed to electrical current, and using a current-voltage converter circuit was monitored as a voltage. The response time of the monitored voltage was measured while applied voltage was varied from 0 to 100 V. We were able to confirm that the monitored voltage followed changes in applied voltage in a highly responsive manner.

We also determined the amount of change in the applied voltage and monitored voltage for a given period of time (0.2 μs), and calculated both the rise time of the voltage at which the rate of change reached a maximum and the time at which the voltages became constant. The time required for the amount of voltage change to reach a maximum was 5.45 and 8.7 μs in the case of applied voltage, and 5.9 and 8.8 μs in the case of monitored voltage. In terms of response time we may assign a value of approximately 0.45 μs.

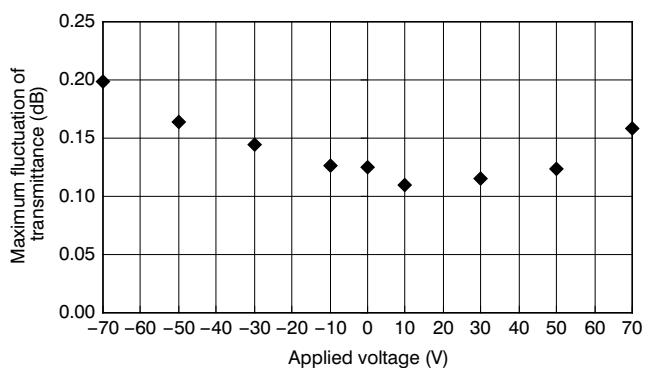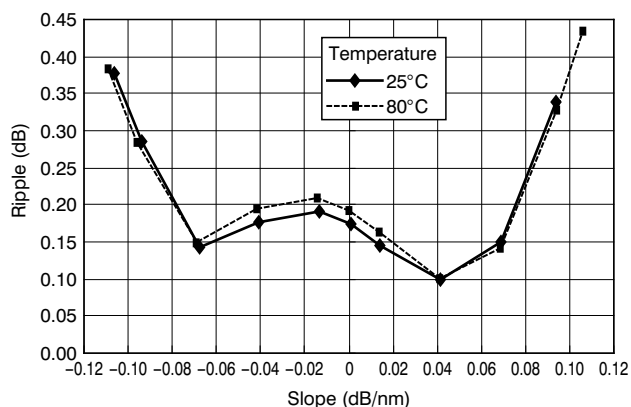Table 1 shows calculated values and the results obtained for the prototyped GTC module. Except for maxi-

Table 1　Characteristics of prototype GTC module.

Item	Calculated value	Measured result
Min. transmittance at center wavelength (dB)	3.3	3.5
Max. ripple (dB)	0.27	0.36
Max. slope voltage (V)	−67	−70.1
Max. slope value (dB/nm)	0.094	0.094
Min. slope voltage (V)	64	68.4
Min. slope value (dB/nm)	−0.093	−0.093
Voltage at 0-dB/nm slope (V)	−1	−0.5
PDL (dB)	—	≤0.1
PMD (ps)	0	0.02
Return loss (dB)	—	>40
Dispersion (ps/nm)	—	+0.6/−0.42
Transition time (μs)	—	0.45
Overall dimensions W × L × H	—	16×72×8.5

mum ripple, the results for the various characteristics were substantially in agreement with the calculated values.

3.5　Temperature Dependence of Characteristics

Figure 15 shows the temperature dependence of transmittance for the prototyped GTC module. The fluctuations in transmittance between 1535 and 1573 nm at voltages of from −70 V to +70 V applied to the module were compared at temperatures of 25, 40, 55, 70, and 80°C and the maximum fluctuation was plotted. Maximum fluctuation

Figure 15　Temperature dependence of transmittance.

Figure 16　Temperature dependence of ripple.

was 0.2 dB at −70 V. Figure 16 shows the temperature dependence of the ripple characteristics for the prototyped GTC module. Measurements were made at temperatures of 25, 40, 55, 70, and 80°C. At a slope of −0.1 dB/nm, the change in ripple was 0.02 dB.

Table 2 shows calculated values and the results obtained for temperature dependence of transmittance and ripple for the prototyped GTC module. Measurements were made at temperatures of 25, 40, 55, 70, and 80°C; calculations were made for temperatures of −5, 10, 25, 40, 55, and 70°C. As Table 2 shows, the measured values were substantially in agreement with the calculated values.
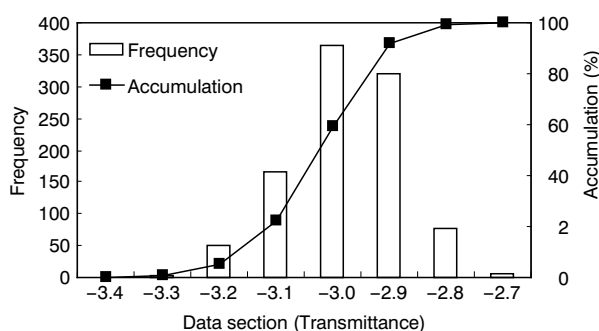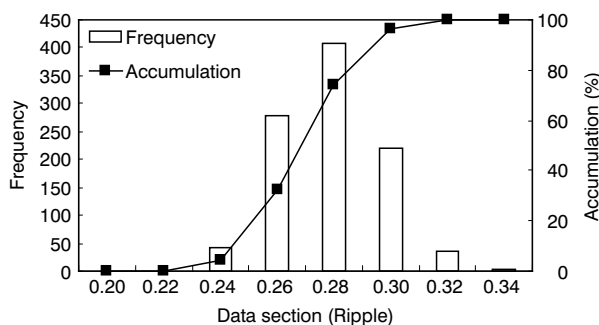
4.　DISCUSSION

The characteristics of the GTC module are impacted by the positioning accuracy of the angle between the crystal axes of its $\lambda/2$ and $\lambda/4$ waveplates and the thickness accuracy of these optical components.

Figures 17 and 18 show the results of simulations of the distribution of transmittance and ripple characteristics for the developed GTC module in the case of random errors of ±1° in axis angle and ±1 nm in thickness for the $\lambda/2$ waveplate (axis angle 22.5°) and $\lambda/4$ waveplate (axis angle 45°).

In this prototype, positioning was accomplished by obtaining the angle of the crystal axes between the wave-

Table 2　Temperature dependence of characteristics (dB).

Item evaluated	Calculated value	Measured result
Max. change in ripple	0.015	0.02
Max. change in loss	0.119	0.2

Figure 17　Result of simulation of transmittance.

Figure 18　Result of simulation of ripple.

plates and one side of their holders. It is estimated that positioning accuracy of the axis angles will be approximately ±1°. The thickness tolerance for the $\lambda/2$ and $\lambda/4$ waveplates was taken as ±1 μm.

For the results shown in Table 1, transmittance at the center wavelength for the developed GTC module was 2.9 dB, when calculated excluding module loss of 0.60 dB. This was within the range of transmittance distribution shown in Figure 17, and is thought to be due to errors in the positioning accuracy or thickness accuracy of the optical components. For ripple, on the other hand, the measured result was 0.36 dB, outside the range for ripple distribution shown in Figure 18. This is attributed to inadequate accuracy in the positioning of the optical components, which needs to be improved.

5. CONCLUSION

To compensate for the millisecond-order gain tilt that is due to the Raman gain changes in the transmission fiber caused by stimulated Raman scattering (SRS) and due to changes in EDFA gain, we have developed a gain tilt compensator using an LN polarization transformer that is capable of microsecond-order operation, and we have confirmed that its transmittance characteristics and response is approximately 0.45 μs.

REFERENCES

1) P. M. Krummrich, et al., "Compensation of Raman transients in optical networks", Technical Digest OFC2004, MF82
2) T. Naito, et al., "Active Gain Compensator in Large-Capacity, Long-Haul WDM Transmission System", Proceedings of OAA'99, Paper WC5
3) H. Hatayama, et al., "Variable attenuation slope compensator (VASC) using silica-based planar lightwave circuit technology for active gain slope control in EDFAs", Technical Digest OFC2000, WH7
4) A. Yariv and P. Yeh, "Optical Waves in Crystals", (Wiley, New York, 1984)